HHS Public Access

Author manuscript

Circ Res. Author manuscript; available in PMC 2018 May 26.

Published in final edited form as:

Circ Res. 2017 May 26; 120(11): 1727–1739. doi:10.1161/CIRCRESAHA.116.309754.

AIBP Limits Angiogenesis Through γ-Secretase-Mediated Upregulation of Notch Signaling

Renfang Mao[1], **Shu Meng**[1], **Qilin Gu**[1], **Raquel Araujo-Gutierrez**[1,2], **Sandeep Kumar**[4], **Qing Yan**[1], **Felicidad Almazan**[5], **Keith A. Youker**[2], **Yingbin Fu**[4], **Henry J. Pownall**[3], **John P. Cooke**[1], **Yury I. Miller**[5], and **Longhou Fang**[1,*]

[1]Center for Cardiovascular Regeneration, Department of Cardiovascular Sciences, 6670 Bertner Avenue, Houston, TX 77030, USA

[2]Houston Methodist DeBakey Heart and Vascular Center, Department of Cardiology, 6670 Bertner Avenue, Houston, TX 77030, USA

[3]Department of Bioenergetics, Houston Methodist Research Institute, 6670 Bertner Avenue, Houston, TX 77030, USA

[4]Department of Ophthalmology, Baylor College of Medicine, Houston, TX77030, USA

[5]Department of Medicine, University of California, San Diego, La Jolla, CA 92093, USA

Abstract

Rationale—Angiogenesis improves perfusion to the ischemic tissue following acute vascular obstruction. Angiogenesis in pathophysiological settings reactivates signaling pathways involved in developmental angiogenesis. We showed previously that apoA-I binding protein (AIBP)-regulated cholesterol efflux in endothelial cells (ECs) controls zebrafish embryonic angiogenesis.

Objective—This study is to determine whether loss of AIBP affects angiogenesis in mice during development and under pathological conditions, and to explore the underlying molecular mechanism.

Methods and Results—In this paper, we report the generation of AIBP knockout (*Apoa1bp*$^{-/-}$) mice, which are characterized of accelerated postnatal retinal angiogenesis. Mechanistically, AIBP triggered relocalization of γ-secretase from lipid rafts to non-lipid rafts where it cleaved Notch. Consistently, AIBP treatment enhanced DLL4-stimulated Notch activation in human retinal ECs. Increasing HDL levels in *Apoa1bp*$^{-/-}$ mice by crossing them with apoA-I transgenic mice rescued Notch activation and corrected dysregulated retinal angiogenesis. Notably, the retinal vessels in

Address correspondence to: Dr. Longhou Fang, Department of Cardiovascular Sciences, Houston Methodist Research Institute, 6670 Bertner Avenue, R10-South, Houston, TX 77030, lhfang@houstonmethodist.org.

AUTHOR CONTRIBUTIONS

L.F, R.M, and Y.I.M conceived the project. L.F and R.M designed the experiments and wrote the manuscript. R.M did the majority of experiments, R.M and S.M. performed hindlimb ischemia experiment in mice under the direction of J.P.C. Q.Y and Q.G did the ISH staining, and F.A conducted experiments in Online Figures I B and C. S.K and Y.F did the experiments in Figure 5E, and R.A and K.Y provided human cardiac tissues. Y.I.M provided constructive suggestions and helped revise the manuscript. H.J.P provided constructive suggestions and experimental materials, helped isolate HDL_3 and together with JPC revised the manuscript. The AIBP knockout mice were generated when L.F was doing his postdoctoral research in the Miller laboratory at UC San Diego.

DISCLOSURES

None.

Apoa1bp$^{-/-}$ mice manifested normal pericyte coverage and vascular integrity. Similarly, in the subcutaneous Matrigel plug assay, which mimics ischemic/inflammatory neovascularization, angiogenesis was dramatically upregulated in *Apoa1bp*$^{-/-}$ mice and associated with a profound inhibition of Notch activation and reduced expression of downstream targets. Furthermore, loss of AIBP increased vascular density and facilitated the recovery of blood vessel perfusion function in a murine hindlimb ischemia model. In addition, AIBP expression was significantly increased in human patients with ischemic cardiomyopathy.

Conclusions—Our data reveal a novel mechanistic connection between AIBP-mediated cholesterol metabolism and Notch signaling, implicating AIBP as a possible druggable target to modulate angiogenesis under pathological conditions.

Keywords

AIBP; cholesterol efflux; lipid rafts; Notch signaling; angiogenesis; cholesterol; lipids and lipoprotein metabolism

Subject Terms

Angiogenesis; Animal Models of Human Disease; Cell Signaling/Signal Transduction; Developmental Biology; Vascular Biology

INTRODUCTION

Angiogenesis, the formation of new blood vessels from preexisting vasculature, mediates delivery of nutrients and oxygen to developing organs while removing metabolic waste products. Angiogenesis requires selection of endothelial tip cells by a gradient of VEGF from the parent vessels, directional migration, and the establishment of connections between new sprouts[1, 2]. Two major signaling pathways, VEGFR and Notch, fine-tune angiogenic sprouting in a reciprocal manner[3–5].

In mammals, the Notch family comprises two Jagged-like ligands (JAG1–2), three Delta-like ligands (DLL1, 3, and 4), and four Notch receptors (Notch1–4)[6–8]. The role of DLL4 and JAG1 during angiogenesis have been well-studied, with DLL4 inhibiting and JAG1 promoting angiogenesis under most developmental or pathological conditions[9–12]. DLL4 is abundant in filopodia-rich tip cells, which respond to surrounding molecular cues. The DLL4 expression, triggered by VEGF[11, 13], activates Notch signaling and suppresses the tip cell phenotype in the neighboring stalk cells. Moreover, DLL4 expression is also induced by Notch[12, 14], which may be a signal-relay mechanism that maintains the stalk cell fate. Notch activation involves a disintegrin and metalloprotease (ADAM)-mediated cleavage at the S2 site, and γ-secretase-mediated cleavage at the S3 site of the Notch receptor generating Notch intracellular domain (NICD), which enters the nucleus to transactivate downstream Notch target gene expression[15–17]. Notch activation downregulates VEGFR2 expression, whereas its suppression augments VEGFR2 signaling and accelerates blood vessel sprouting and branching[6, 9, 18–22].

Our recent study uncovered a previously unrecognized connection between cholesterol metabolism and blood vessel formation in zebrafish. Cholesterol transport requires cholesterol transporters ATP-binding cassette (ABC) family members ABCA1 and ABCG1; ABCA1 mediates cholesterol efflux to the lipid-poor cholesterol acceptor apoA-I, yielding a nascent HDL, while ABCG1 mediates cholesterol efflux to mature HDL[23–26]. We showed that spatiotemporal expression of AIBP restrains and guides angiogenesis in embryonic zebrafish. Mechanistically, AIBP accelerates cholesterol efflux from ECs to HDL, which in turn reduces the amount of plasma membrane cholesterol available for lipid raft formation, thereby impairing VEGFR2 signaling competence[27]. Extracellular AIBP promotes cholesterol efflux from human macrophages, thereby reducing lipid accretion[28]. AIBP, encoded by the *Apoa1bp* gene in mice and *APOA1BP* gene in humans, is a secreted protein that physically associates with apoA-I[29]; AIBP is ubiquitously expressed and abundant in most human organs with secretory functions. Of note, AIBP is not expressed in the skeletal muscle but is highly expressed in vascular smooth muscle cells and in heart muscle[30], which implicates AIBP in cardiovascular functions. AIBP is evolutionarily conserved from Drosophila to human[29, 31], thus we propose that the role of AIBP in angiogenesis is also conserved from zebrafish to mice to humans. Importantly, understanding the molecular mechanism for AIBP-regulated angiogenesis may guide the development of novel therapeutic strategies targeting angiogenesis in different pathological settings. To this end, we generated *Apoa1bp*$^{-/-}$ mice with which we discovered a new mechanistic underpinning of AIBP-regulated angiogenesis, which downregulates Notch in a γ-secretase-dependent fashion and restricts murine retinal and pathological angiogenesis. Importantly, loss of AIBP accelerates angiogenesis without affecting the integrity and functionality of blood vessels, suggesting that AIBP is a potential pharmacological target for treating cardiovascular disease.

METHODS

Preparation of whole mount retinas

After euthanization, eyes of neonatal mice at the appropriate developmental stage were isolated, fixed in 4% paraformaldehyde (PFA) and dissected. Retinal cups were subjected to immunostaining with the indicated Abs or extraction of total RNA or proteins as described below.

In situ hybridization (ISH)

Murine retinas were incubated sequentially in 15% sucrose-PBS, 30% sucrose-PBS, and OCT, and then used to prepare 5 μm-thick sections. After fixation in 4% PFA and acetylation in 1% triethanolamine and 0.25% acetic anhydride, the slides were prehybridized and incubated overnight with hybridization solution containing the RNA probes at 65°C. Subsequently, the sections were washed and probed with AP-conjugated anti-DIG Ab or anti-fluorescein Ab. The sections were developed with the addition of fast red or NBT/BCIP substrate. For double-probe ISH, both digoxigenin-incorporated *Apoa1bp* and fluorescein-incorporated *Brn3* were hybridized with the same section, and the sections were then first incubated with AP-conjugated anti-digoxigenin antibody, for which NBT/BCIP was used as a chromogenic substrate. Subsequently, the sections were washed and post fixed with 4%

PFA and further incubated with AP-conjugated anti-fluorescein antibody, and developed with fast red (Roche). The Brn3b plasmid for making the riboprobe was kindly provided by Dr. Chenghua Gu (Harvard Medical School).

Retinal whole mount immunostaining

Retinas were PFA-fixed, permeabilized and blocked in TBST containing 1% BSA and 5% goat or donkey serum. After three washes with Pblec buffer (0.5% Triton X-100, 1 mM $CaCl_2$, 1 mM $MgCl_2$, and 1 mM $MnCl_2$ in PBS, pH 6.8), the retinas were incubated overnight with primary antibodies diluted in the blocking solution at 4°C. The following primary Abs were used: rat anti-CD31 (1:200, BD Biosciences), rabbit anti-Collagen IV (1:250, Millipore), and rabbit anti-NG2 (1:250, Millipore). The secondary Abs were Alexa Fluor@−488 or −594 conjugated anti-rat or anti-rabbit IgGs (1:500, Jackson ImmunoResearch). After antibody staining, retinas were post-fixed in 4% PFA for 15 min and then were flat-mounted under a dissecting microscope. Images were captured using Olympus Fluoview FV1000 Laser Scan Confocal Microscope. The acquired images were quantified for retinal vascular density, numbers of tip cells, and filopodia as previously described[32] using Image J (National Institutes of Health).

H&E and Immunohistochemistry (IHC)

The PFA-fixed Matrigel plug was washed in PBS and then embedded in paraffin. Five-micrometer sections were prepared, deparaffinized by sequential incubation in xylene and ethanol. After rehydration, the slides were stained with hematoxylin and eosin following a standard protocol.

For IHC staining of Matrigel plugs harvested from the mice, 5 μm-thick paraffin sections were deparaffinized, hydrated, and boiled in 10 mM sodium citrate buffer (pH 6.0) for 15 min to facilitate antigen retrieval. After a brief treatment with Background Buster Blocking Agent (Innovex Biosciences), the slides were incubated with the primary antibody for 45 min. After washing, the slides were incubated sequentially with STAT-Q secondary linking antibodies (Innovex Biosciences), HRP-labeled streptavidin and Innovex substrate (DAB) for color development following the manufacturer's instructions.

DLL4-induced NICD production

Human retinal ECs were plated and kept in culture for 4 hours onto 6-well plates that were pre-coated with or without recombinant human DLL4 protein (0.5 μg/ml) in 0.1% BSA/PBS for 1 hour at room temperature. Cells were further incubated with AIBP (0.1 μg/ml), HDL_3 (50 μg/ml), or their combination for 4 hours, with 20 μM DAPT (γ-secretase inhibitor) for 24 hours, 10mM MβCD for 10 min or 10 μg/ml water soluble cholesterol (Sigma) for 2 hours. After the various treatments, cells were washed with PBS and lysed. The NICD levels were assessed by western blot using a γ-secretase cleavage-specific antibody Val1744 (Cell Signaling Technology)

RESULTS

AIBP expression in the retinal ganglion cells

Apoa1bp-null mice were generated as described (Online Figure IA); PCR and western blot analysis indicated the absence of AIBP (Online Figure I B–D). AIBP-null mice are viable and fertile, and have no apparent morphological defects compared to control mice under naïve conditions. Our study in zebrafish showed that Aibp functions non-cell autonomously in angiogenesis[27], and that the tissue localization of Aibp at 24 hours post fertilization is similar to that of Sema 3a[33]. To assess the mRNA localization of murine *Apoa1bp*, in situ hybridization (ISH) was performed on adjacent sections through postnatal day 5 (P5) murine retinas for *Apoa1bp* and *Brn3b*, a retinal ganglion cell (RGC) marker. As with our study in zebrafish, *Apoa1bp* mRNA was localized in the *Brn3b*-positive RGC layer of a murine retina (Online Figure II), which expresses *Sema3E*[34]. As expected, the *Apoa1bp* mRNA signal was absent in the *Apoa1bp* knockout retina (Online Figure IIA and IIC). AIBP expression in RGC implies a paracrine role of AIBP in murine retinal angiogenesis.

Loss of AIBP increases murine retinal angiogenesis

We assessed AIBP function in the retinal vasculature. The murine retina is avascular at birth; starting from postnatal day 1 (P1), a single superficial layer of blood vessels extends radially outwards from the center vessels at the optical nerve head toward the periphery until P7[35]. Whole-mount immunofluorescent staining of the isolated retinas was performed with CD31 and Collagen IV on P5 retinas. AIBP-deficient retinas at P5 showed a profound increase in the radial extension of vascular plexus from the optic nerve to the periphery (Figure 1A and 1B) and in the total vascular area (Figure 1A and 1C). Next, we analyzed the branch points in *Apoa1bp*$^{-/-}$ and control littermates since extensive remodeling and sprouting is required to establish an interconnected vasculature network. The front and center areas analyzed in the retinas are illustrated in Figure 1D. Consistent with a role for AIBP in retinal angiogenesis, more branch points were observed in both front and central areas of the vascular plexus in the *Apoa1bp*$^{-/-}$ retinas compared to control littermate retinas (Figure 1E–1G). Similar results were obtained in P3 neonates' retinas (Online Figure III A). During angiogenesis, tip cells manifest exploratory and sprouting behavior by extending numerous filopodia[1]. More endothelial tip cells were observed in AIBP null retinas than that in control littermates (Figure 2H and 2I), and the number of filopodia was significantly increased in *Apoa1bp*$^{-/-}$ retinas (Figure 1J and 1K). However, loss of AIBP had no effect on blood vessel formation at P7 and P9 (Online Figure III B and C), which indicates that AIBP disruption accelerates normal retinal angiogenesis. The difference in angiogenesis may be caused by change in vessel stability. Thus, we stained for Collagen IV because regressed vessels generally leave empty sleeves of collagen IV-rich matrix deposits and which are used for the assessment of vessel stability[36]. There was no apparent difference in vessel stability because similar numbers of empty sleeves (Col IV^{+}CD31^{-}) were found in the AIBP knockout and control mice (Online Figure IV A and B). Collectively, AIBP deficiency in mice results in significantly accelerated angiogenesis as evidenced by a greater radial extension length of vascular plexus, the development of a denser upper capillary layer, and a higher number of tip cells, as well as filopodia, in the retinas. This phenotype is however normalized by P7.

AIBP controls Notch signaling in murine retinas

Given that Notch signaling suppresses angiogenesis in most vascular beds[37, 38], we determined whether accelerated retinal angiogenesis in *Apoa1bp*$^{-/-}$ mice was due to impaired Notch activity. The activation of the Notch pathway was markedly attenuated as evidenced by diminished production of NICD levels in *Apoa1bp*$^{-/-}$ retinas (Figure 2A and 2B). Expression of *Hey1*, a transcriptional repressor of Notch that is selectively expressed in the blood vessels during retinal angiogenesis[6, 39], *Hey2*, and *Hes1* were significantly decreased in P5 (Figure 2C) and P3 (Figure 2D) *Apoa1bp*$^{-/-}$ retinas. However, Notch receptors (*Notch1* and *Notch4*), Notch ligand *Dll4*, and Notch pathway negative regulator *Nrarp* mRNA showed no significant change in P5 or P3 retinas (Online Figure V A and B). Consistent with this finding, the Notch1 protein levels were comparable between *Apoa1bp*$^{-/-}$ and control retinas (Online Figure V C and D). As expected, AIBP deficiency augmented VEGFR2 activation (Figure 2A, Online Figure V C and D), but did not affect *Vegfa* gene expression (Online Figure V A and B). These results indicate that loss of AIBP suppresses Notch signaling in postnatal murine retinas. Collectively, our results provide compelling support for the hypothesis that AIBP positively regulates Notch signaling, thereby restricting angiogenesis.

We have previously shown that AIBP controls angiogenesis via a direct effect on VEGFR2 localization to cholesterol-rich lipid rafts[27]. To distinguish the role of AIBP in VEGFR2 and Notch pathways, control and *Apoa1bp*$^{-/-}$ mice were treated with the Notch inhibitor DAPT and retinal angiogenesis was assessed. DAPT inhibited retinal angiogenesis in *Apoa1bp*$^{-/-}$ mice to a significantly lesser degree than in control mice (Online Figure VI). These data indicate that AIBP regulates retinal angiogenesis through both Notch–dependent and –independent pathways.

AIBP exerts its effect via γ-secretase-regulated Notch signaling

Binding of a Notch ligand to a Notch receptor initiates two cleavage steps that generate transcriptionally active NICD—the first step mediated by ADAM and the second by γ-secretase[40]. Since AIBP deficiency has no effect on Notch1 protein levels (Online Figure V C and D), and our previous studies showed that AIBP-mediated depletion of cholesterol disrupts lipid rafts[27], we tested whether AIBP exerts its effect on γ-secretase-regulated Notch via alteration of lipid rafts. The γ-secretase complex, which includes the four proteins presenilin1, nicastrin, anterior pharynx defective1, and presenilin enhancer 2[41–43], is localized to plasma membrane lipid rafts. Disruption of lipid rafts by modest cholesterol reduction induces γ-secretase translocation from lipid rafts to non-rafts, which augments the cleavage of its substrate, amyloid precursor protein (APP), in neurons[44]. Therefore, we postulated that AIBP-mediated reduction of lipid raft abundance also enhances Notch cleavage via effects on γ-secretase distribution in ECs. We reasoned that AIBP may interact with cells to achieve an effect on lipid rafts. Thus, we verified the binding of AIBP to human retinal microvascular endothelial cells (HRMECs) (Online Figure VII). Next, we performed detergent-free, discontinuous gradient ultracentrifugation analysis of HRMECs treated with control media, AIBP, HDL_3, or their combination, and found that co-incubation with AIBP and HDL_3 translocated γ-secretase and Notch1 from lipid rafts to non-raft domains (Figure 3A).

Previous studies suggest that lipid rafts regulate γ-secretase[45]. Thus, we examined the effect of cholesterol on DLL4-stimulated Notch activity by incubating HRMECs with methyl-β-cyclodextrin (MβCD), an efficient cholesterol sequestrant, for 0 to 60 min. MβCD treatment markedly increased NICD production, peaking at 10–15 min and returning to near basal levels at 60 min (Figure 3B and 3C). As expected, the NICD levels roughly correlated with the amount of cholesterol extracted from cells by MβCD (Figure 3C). We next examined the effect of AIBP on DLL4-induced Notch activity in human ECs. HRMECs were incubated with AIBP, HDL_3, or both. Coincubation with AIBP and HDL_3, but not alone, significantly increased DLL4-stimuated NICD production (Figure 3D and 3E). In contrast, supplementation of cells with free cholesterol completely eliminated NICD generation (Figure 3D). As expected, the γ-secretase inhibitor DAPT abolished the production of NICD (Figure 3D and 3E). To further test the effect of lipid rafts on γ-secretase-mediated Notch signaling, a truncated version of Notch (NotchΔE) lacking the extracellular domain but retaining the γ-secretase cleavage site[46], was transfected into HEK293T cells, followed by AIBP treatment in the presence or absence of HDL_3. We found that AIBP and HDL_3 in combination, but not alone, increased the γ-secretase-dependent generation of NICD from NotchΔE (Figure 3F and 3G). As in human ECs, treatment with MβCD or DAPT augmented or suppressed Notch activation, respectively (Figure 3F and 3G). Together these results indicate that AIBP/HDL_3 positively regulates Notch signaling by directing γ-secretase and Notch from lipid rafts to non-lipid domains, where enhanced γ-secretase-mediated Notch cleavage occurs.

Increasing HDL levels rescues dysregulated retinal angiogenesis in AIBP null mice

We showed that AIBP-mediated cholesterol efflux increased Notch activity (Figure 3B–3G), an effect achieved through reduction of lipid raft abundance. The apoA-I transgenic mice (*Apoa1*^{Tg}), which have approximately 2-fold higher levels of HDL-cholesterol than controls[47], were used to correct the myeloproliferative disorder caused by increased lipid rafts in mice with a deficiency of the cholesterol transporters, ABCA1 and ABCG1[48]. Therefore, we crossed *Apoa1bp*$^{-/-}$ mice with apoA-I transgenic mice to increase HDL levels in *Apoa1bp*$^{-/-}$ mice, and determined the effect of increased HDL levels on dysregulated angiogenesis in *Apoa1bp* knockout retinas (Online Figure VIII A and B). As expected, increased HDL levels in AIBP null retinas reversed the proangiogenic phenotype, including the radial extension of vascular plexus (Figure 4A–4C), vascular branch points (Figure 4D–4F), number of tip cells, and filopodia in the retinas (Figure 4G–4J). Consistent with this, increasing HDL levels reduced VEGFR2 activation in *Apoa1bp*$^{-/-}$ retinas (Online Figure VIIIC). We observed no changes in vessel remodeling based on similar numbers of empty sleeves in the P5 retinas of *Apoa1bp*$^{-/-}$ and *Apoa1bp*$^{-/-}$*Apoa1*^{Tg} mice (Online Figure IX). To assess whether Notch activity is enhanced in *Apoa1*^{Tg} mice, NICD protein levels were probed in *Apoa1bp*$^{-/-}$ and *Apoa1bp*$^{-/-}$*Apoa1*^{Tg} retinas. As illustrated in Figures 4K, 4L, and Online Figure VIII A, NICD levels were elevated, and VEGFR2 phosphorylation was reduced in *Apoa1bp* null mice with apoA-I overexpression. In addition, quantitative real time PCR (qRT-PCR) analysis was performed to assess the expression of Notch receptors and ligands, as well as downstream target genes. *Hey1*, *Hey2*, and *Hes1* mRNA levels were significantly increased at P5 in the retinas from *Apoa1bp*$^{-/-}$*Apoa1*^{Tg} compared with that of

Apoa1bp$^{-/-}$ (Figure 4M). Increased HDL levels had no significant effect on *Notch1*, *Notch4*, *Dll4, Nrarp* or *Vegfa* gene expression (Online Figure VIIID).

Vascular permeability and pericyte coverage in AIBP knockout mice

Our data indicate that the loss of AIBP accelerates developmental angiogenesis, which might be beneficial in patients with tissue ischemia. To explore the potential of AIBP for therapeutic purposes, we determined whether loss of AIBP affects perfusion and vasculature leakage. Adequate pericyte coverage is essential for the integrity of blood vessels. Therefore, mural cell coverage of ECs was investigated by whole mount immunofluorescence staining of NG2 and CD31 in P5 retinas. We found no difference in pericyte coverage in both front and central regions of P5 retinas between *Apoa1bp*$^{-/-}$ and control littermate neonatal mice (Figure 5A–5D).

To further determine the effect of AIBP on vascular integrity in vivo, we performed fluorescein angiography on *Apoa1bp*$^{-/-}$ and control WT mice. Neither the *Apoa1bp*$^{-/-}$ mice nor the control WT littermates showed any retinal vascular leakage (Figure 5E). Collectively, our data suggest that loss of AIBP accelerates angiogenesis while retaining vascular integrity.

Loss of AIBP in mice enhances neovascularization in the Matrigel plug assay and improves functional recovery of the vasculature in the murine hindlimb ischemia model

To test the effect of AIBP absence on in vivo angiogenesis under conditions simulating a pathological process, we injected Matrigel into a subcutaneous location. The Matrigel hardens into a plug, which is invaded by immune cells and becomes vascularized. This is a model of neovascularization occurring with ischemia and inflammation. Five days after injection, the Matrigel plugs were retrieved, and H&E and IHC were performed to evaluate blood vessel formation and perfusion within the plugs. As expected, there were more blood vessels in Matrigel plugs from *Apoa1bp*$^{-/-}$ mice than that from control mice (Figure 6A–6C). Quantitative RT-PCR analysis confirmed that expression of EC markers CD31 and VE-cadherin was significantly increased in Matrigel plugs from *Apoa1bp*$^{-/-}$ mice (Figure 6D and 6E). These data indicate that AIBP inhibits inflammatory neovascularization in mice, which agrees with the results of accelerated postnatal retinal angiogenesis. Remarkably, the effect of AIBP ablation on Matrigel neovascularization was more robust than in retinal angiogenesis, suggesting an important role of AIBP in regulation of angiogenesis under pathologic conditions.

Next we examined whether enhanced pathological angiogenesis in *Apoa1bp*$^{-/-}$ mice was due to attenuated Notch activity. Western blot analysis revealed significantly reduced NICD levels in Matrigel plugs from *Apoa1bp*$^{-/-}$ mice (Figure 6F and 6G). Moreover, expression of Notch downstream target genes *Hey1*, *Hey2*, and *Hes1* was drastically reduced in Matrigel plugs from *Apoa1bp*$^{-/-}$ mice (Figure 6H), whereas *Notch1* and *Notch4*, *Dll4*, and *Nrarp* mRNA levels showed no significant change (Online Figure X). These results suggest that AIBP inhibits angiogenesis via positive regulation of Notch activity.

To further assess the role of AIBP in pathological angiogenesis, we used the murine hindlimb ischemia model. In unoperated animals, similar values of limb perfusion were

observed in WT and AIBP knockout mice using laser Doppler imaging (Figure. 7A). However, after induction of limb ischemia by femoral artery ligation, the increase in gastrocnemius capillary density and the recovery of limb perfusion was significantly enhanced in the AIBP knockout animals (Figure 7A–D). The results suggest that AIBP deficiency promotes functional blood vessel formation.

Increased AIBP expression in human ischemic cardiomyopathy

Augmented angiogenesis promotes cardiac recovery following ischemia[49–51]. To extend our findings on AIBP to the context of human cardiomyopathy, we analyzed AIBP expression in normal hearts or in hearts from patients with ischemic cardiomyopathy (ICM). Interestingly, AIBP expression was markedly increased in the myocardial tissue from ICM patients by comparison to that from patients without ICM (Figure 8). The data imply a possible role of AIBP in ICM where increased AIBP expression may contribute to the ischemic pathophysiology.

DISCUSSION

Here we showed that AIBP suppresses angiogenesis via enhanced Notch activity. AIBP knockout in mice increased postnatal retinal angiogenesis, augmented neovascularization in subcutaneous Matrigel plugs and enhanced the increase in capillary density and recovery of limb perfusion in the murine hindlimb ischemia model (Figure 1, 6 and 7). Moreover, we revealed that AIBP-triggered lipid raft content reduction enhances the codistribution of γ-secretase and Notch in non-lipid raft fraction, and subsequently increases the γ-secretase-mediated cleavage of Notch1, thereby augmenting Notch activity (Figure 3). Our study connects AIBP-regulated cholesterol content in the plasma membrane with Notch signaling, which extends our findings in zebrafish and implies the conserved role of AIBP in angiogenesis. More importantly, we showed that loss of AIBP does not influence vascular integrity and that accelerated angiogenesis in *Apoa1bp*$^{-/-}$ mice produces functional blood vessels (Figure 5). Interestingly, AIBP expression is substantially elevated in patients with ICM (Figure 8), suggesting that AIBP may be a novel determinant of tissue ischemia. Our findings indicate that AIBP may be a pharmacologic target for cardiovascular therapeutics.

AIBP effect on developmental and pathological angiogenesis

The human *APOA1BP* gene is located at 1q21.2-1q22, which corresponds to the 1q21-q23 locus for familial combined hyperlipidemia, a common, multifactorial, and heterogeneous dyslipidemia predisposing individuals to premature coronary artery disease[52]. Despite this observation, there are no studies linking AIBP polymorphism with dyslipidemia or risk of cardiovascular disease[53]. Our study is the first to identify a non-cell autonomous role of AIBP in angiogenesis.

Pathological angiogenesis usually recapitulates certain features of developmental angiogenesis[54–56]. In our Matrigel experiment, which simulates some aspects of pathological angiogenesis, AIBP exerted a striking effect on regulating Notch and angiogenesis (Figure 6). However, the effect of AIBP on Notch in postnatal retinal angiogenesis was modest (Figure 1), which may be due to the more acute nature of

Matrigel-induced pathological angiogenesis that amplifies the function of AIBP in regulating Notch (Figure 6).

Lipid rafts, γ-secretase and Notch

Lipid rafts are implicated in the regulation of γ-secretase activity, which cleaves Notch thereby activating its signaling. γ-secretase seems to manifest greater activity in lipid rafts in in vitro studies[57] and facilitates the cleavage of its substrate APP[58]. On the other hand, lowering brain cholesterol levels in mice using statins increases amyloid production[59]. Further, in human patients with a genetic mutation that causes cellular cholesterol accumulation, early onset of APP aggregation is also found[60, 61]. Notably, γ-secretase is located in non-lipid raft membranes during embryonic development, but in lipid rafts in adults[62]. These three pieces of evidence suggest that reduction of lipid raft levels does not necessarily lead to an effect that is associated with decreased γ-secretase activity. Rather, in cultured neurons, a modest reduction of lipid raft abundance confers enhanced cleavage of APP by γ-secretase in non-raft fractions[44]. In support of this, our results indicate that AIBP/HDL_3 treatment relocates γ-secretase from the lipid raft fractions to the non-raft fractions; this precipitates codistribution of γ-secretase with Notch1 in the non-raft fractions and enhances Notch signaling (Figure 3). Thus, our study uncovered a new molecular mechanism by which AIBP regulates angiogenesis via its effect on γ-secretase-mediated Notch signaling. Our results suggest that AIBP acts primarily on Notch receptor proteolytic processing since qRT-PCR and immunoblotting analysis indicated no substantial expression change of DLL4 and Notch1 in murine retinas (Online Figure V, VIIID, and X). Taken together, these results support a model in which AIBP regulates angiogenesis through its effect on γ-secretase translocation from lipid rafts to non-lipid rafts and ensuing Notch cleavage (Online Figure XI).

AIBP-regulated angiogenesis and vascular integrity

In addition to identifying the inhibitory role of AIBP in angiogenesis, we also assessed the effect of AIBP on vascular integrity and permeability. We showed that in contrast to excessive VEGF treatment[55] or Epsin deficiency,[63] which promotes nonfunctional angiogenesis and results in a leaky vasculature, loss of AIBP augments functional vasculature formation, as illustrated by normal extent of pericyte coverage and undetectable fluorescein leakage (Figure 5). Furthermore, we showed that AIBP-deficiency facilitated blood vessel formation and improved the functional recovery of vasculature in a murine hindlimb ischemia model, which suggests the possibility of an AIBP-based therapy for angiogenesis-associated diseases. Given that stimulation of angiogenesis is considered beneficial for the treatment of myocardial infarction, and that AIBP is markedly increased under the ICM condition (Figure 8), it will be interesting to determine whether targeting AIBP is salutary for ICM.

Supplementary Material

Refer to Web version on PubMed Central for supplementary material.

Acknowledgments

We thank Drs Ju Chen and Jianlin Zhang for the help on the generation of Apoa1bp-floxed and knockout mice. We thank Dr. Chenghua Gu (Harvard Medical School) for providing the plasmid for making *Brn3* RNA probe. We thank Drs Pingwen Xu and Rong Xu (Baylor College of Medicine) for help on the ISH. We thank Dr. Pengchun Yu at Yale School of Medicine, and Drs Baiba Gillard, and Li Lai at Houston Methodist Research Institute (HMRI) for helpful disscussions and technical support. We also thank the research pathology core and advanced cellular and tissue microscopy core at HMRI for excellent services. We thank Dr. Johnique Atkins for manuscript editing.

SOURCES OF FUNDING

This study was supported by grants from the NIH (HL114734 and HL132155), AHA (16BGIA27790081), and startup funds from HMRI to L.F, and the NIH grants HL135737 (Y.I.M), HL129767 (H.J.P), U01 HL100397 (J.P.C), and AHA postdoctoral fellowship 17POST33410128 (R.M).

Nonstandard Abbreviations and Acronyms

AIBP	apoA-I binding protein
HDL	high-density lipoprotein
ABC	ATP-binding cassette
ECs	endothelial cells
CD31	cluster of differentiation 31 protein
NICD	Notch1 intracellular domain
HRMECs	human retinal microvascular endothelial cells
ADAM	a disintegrin and metalloprotease
MβCD	methyl-β-cyclodextrin
ICM	ischemic cardiomyopathy
WT	wild-type

References

1. Gerhardt H, Golding M, Fruttiger M, Ruhrberg C, Lundkvist A, Abramsson A, Jeltsch M, Mitchell C, Alitalo K, Shima D, Betsholtz C. VEGF guides angiogenic sprouting utilizing endothelial tip cell filopodia. J Cell Biol. 2003; 161:1163–77. [PubMed: 12810700]
2. De Smet F, Segura I, De Bock K, Hohensinner PJ, Carmeliet P. Mechanisms of vessel branching: filopodia on endothelial tip cells lead the way. Arterioscler Thromb Vasc Biol. 2009; 29:639–49. [PubMed: 19265031]
3. Roca C, Adams RH. Regulation of vascular morphogenesis by Notch signaling. Genes Dev. 2007; 21:2511–24. [PubMed: 17938237]
4. Ferrara N, Gerber HP, LeCouter J. The biology of VEGF and its receptors. Nat Med. 2003; 9:669–76. [PubMed: 12778165]
5. Lohela M, Bry M, Tammela T, Alitalo K. VEGFs and receptors involved in angiogenesis versus lymphangiogenesis. Curr Opin Cell Biol. 2009; 21:154–65. [PubMed: 19230644]
6. Benedito R, Roca C, Sorensen I, Adams S, Gossler A, Fruttiger M, Adams RH. The notch ligands Dll4 and Jagged1 have opposing effects on angiogenesis. Cell. 2009; 137:1124–35. [PubMed: 19524514]

7. Bray SJ. Notch signalling: a simple pathway becomes complex. Nat Rev Mol Cell Biol. 2006; 7:678–89. [PubMed: 16921404]
8. Herbert SP, Stainier DY. Molecular control of endothelial cell behaviour during blood vessel morphogenesis. Nat Rev Mol Cell Biol. 2011; 12:551–64. [PubMed: 21860391]
9. Siekmann AF, Lawson ND. Notch signalling limits angiogenic cell behaviour in developing zebrafish arteries. Nature. 2007; 445:781–4. [PubMed: 17259972]
10. Suchting S, Freitas C, le Noble F, Benedito R, Breant C, Duarte A, Eichmann A. The Notch ligand Delta-like 4 negatively regulates endothelial tip cell formation and vessel branching. Proc Natl Acad Sci U S A. 2007; 104:3225–30. [PubMed: 17296941]
11. Noguera-Troise I, Daly C, Papadopoulos NJ, Coetzee S, Boland P, Gale NW, Lin HC, Yancopoulos GD, Thurston G. Blockade of Dll4 inhibits tumour growth by promoting non-productive angiogenesis. Nature. 2006; 444:1032–7. [PubMed: 17183313]
12. Ridgway J, Zhang G, Wu Y, Stawicki S, Liang WC, Chanthery Y, Kowalski J, Watts RJ, Callahan C, Kasman I, Singh M, Chien M, Tan C, Hongo JA, de Sauvage F, Plowman G, Yan M. Inhibition of Dll4 signalling inhibits tumour growth by deregulating angiogenesis. Nature. 2006; 444:1083–7. [PubMed: 17183323]
13. Lobov IB, Renard RA, Papadopoulos N, Gale NW, Thurston G, Yancopoulos GD, Wiegand SJ. Delta-like ligand 4 (Dll4) is induced by VEGF as a negative regulator of angiogenic sprouting. Proc Natl Acad Sci U S A. 2007; 104:3219–24. [PubMed: 17296940]
14. Shawber CJ, Das I, Francisco E, Kitajewski J. Notch signaling in primary endothelial cells. Ann N Y Acad Sci. 2003; 995:162–70. [PubMed: 12814948]
15. Mumm JS, Schroeter EH, Saxena MT, Griesemer A, Tian X, Pan DJ, Ray WJ, Kopan R. A ligand-induced extracellular cleavage regulates gamma-secretase-like proteolytic activation of Notch1. Mol Cell. 2000; 5:197–206. [PubMed: 10882062]
16. Bozkulak EC, Weinmaster G. Selective use of ADAM10 and ADAM17 in activation of Notch1 signaling. Mol Cell Biol. 2009; 29:5679–95. [PubMed: 19704010]
17. Brou C, Logeat F, Gupta N, Bessia C, LeBail O, Doedens JR, Cumano A, Roux P, Black RA, Israel A. A novel proteolytic cleavage involved in Notch signaling: the role of the disintegrin-metalloprotease TACE. Mol Cell. 2000; 5:207–16. [PubMed: 10882063]
18. Gridley T. Vascular biology: vessel guidance. Nature. 2007; 445:722–3. [PubMed: 17301780]
19. Li JL, Harris AL. Notch signaling from tumor cells: a new mechanism of angiogenesis. Cancer Cell. 2005; 8:1–3. [PubMed: 16023591]
20. Phng LK, Gerhardt H. Angiogenesis: a team effort coordinated by notch. Dev Cell. 2009; 16:196–208. [PubMed: 19217422]
21. Hellstrom M, Phng LK, Hofmann JJ, Wallgard E, Coultas L, Lindblom P, Alva J, Nilsson AK, Karlsson L, Gaiano N, Yoon K, Rossant J, Iruela-Arispe ML, Kalen M, Gerhardt H, Betsholtz C. Dll4 signalling through Notch1 regulates formation of tip cells during angiogenesis. Nature. 2007; 445:776–80. [PubMed: 17259973]
22. Tammela T, Zarkada G, Wallgard E, Murtomaki A, Suchting S, Wirzenius M, Waltari M, Hellstrom M, Schomber T, Peltonen R, Freitas C, Duarte A, Isoniemi H, Laakkonen P, Christofori G, Yla-Herttuala S, Shibuya M, Pytowski B, Eichmann A, Betsholtz C, Alitalo K. Blocking VEGFR-3 suppresses angiogenic sprouting and vascular network formation. Nature. 2008; 454:656–60. [PubMed: 18594512]
23. Wang N, Silver DL, Thiele C, Tall AR. ATP-binding cassette transporter A1 (ABCA1) functions as a cholesterol efflux regulatory protein. J Biol Chem. 2001; 276:23742–7. [PubMed: 11309399]
24. Bodzioch M, Orso E, Klucken J, Langmann T, Bottcher A, Diederich W, Drobnik W, Barlage S, Buchler C, Porsch-Ozcurumez M, Kaminski WE, Hahmann HW, Oette K, Rothe G, Aslanidis C, Lackner KJ, Schmitz G. The gene encoding ATP-binding cassette transporter 1 is mutated in Tangier disease. Nat Genet. 1999; 22:347–51. [PubMed: 10431237]
25. Klucken J, Buchler C, Orso E, Kaminski WE, Porsch-Ozcurumez M, Liebisch G, Kapinsky M, Diederich W, Drobnik W, Dean M, Allikmets R, Schmitz G. ABCG1 (ABC8), the human homolog of the Drosophila white gene, is a regulator of macrophage cholesterol and phospholipid transport. Proc Natl Acad Sci U S A. 2000; 97:817–22. [PubMed: 10639163]

26. Kennedy MA, Barrera GC, Nakamura K, Baldan A, Tarr P, Fishbein MC, Frank J, Francone OL, Edwards PA. ABCG1 has a critical role in mediating cholesterol efflux to HDL and preventing cellular lipid accumulation. Cell Metab. 2005; 1:121–31. [PubMed: 16054053]
27. Fang L, Choi SH, Baek JS, Liu C, Almazan F, Ulrich F, Wiesner P, Taleb A, Deer E, Pattison J, Torres-Vazquez J, Li AC, Miller YI. Control of angiogenesis by AIBP-mediated cholesterol efflux. Nature. 2013; 498:118–22. [PubMed: 23719382]
28. Zhang M, Li L, Xie W, Wu JF, Yao F, Tan YL, Xia XD, Liu XY, Liu D, Lan G, Zeng MY, Gong D, Cheng HP, Huang C, Zhao ZW, Zheng XL, Tang CK. Apolipoprotein A-1 binding protein promotes macrophage cholesterol efflux by facilitating apolipoprotein A-1 binding to ABCA1 and preventing ABCA1 degradation. Atherosclerosis. 2016; 248:149–59. [PubMed: 27017521]
29. Ritter M, Buechler C, Boettcher A, Barlage S, Schmitz-Madry A, Orso E, Bared SM, Schmiedeknecht G, Baehr CH, Fricker G, Schmitz G. Cloning and characterization of a novel apolipoprotein A-I binding protein, AI-BP, secreted by cells of the kidney proximal tubules in response to HDL or ApoA-I. Genomics. 2002; 79:693–702. [PubMed: 11991719]
30. Wilhelm M, Schlegl J, Hahne H, Moghaddas Gholami A, Lieberenz M, Savitski MM, Ziegler E, Butzmann L, Gessulat S, Marx H, Mathieson T, Lemeer S, Schnatbaum K, Reimer U, Wenschuh H, Mollenhauer M, Slotta-Huspenina J, Boese JH, Bantscheff M, Gerstmair A, Faerber F, Kuster B. Mass-spectrometry-based draft of the human proteome. Nature. 2014; 509:582–7. [PubMed: 24870543]
31. Fang L, Miller YI. Targeted cholesterol efflux. Cell Cycle. 2013; 12:3345–6. [PubMed: 24036659]
32. Pitulescu ME, Schmidt I, Benedito R, Adams RH. Inducible gene targeting in the neonatal vasculature and analysis of retinal angiogenesis in mice. Nat Protoc. 2010; 5:1518–34. [PubMed: 20725067]
33. Torres-Vazquez J, Gitler AD, Fraser SD, Berk JD, Van NP, Fishman MC, Childs S, Epstein JA, Weinstein BM. Semaphorin-plexin signaling guides patterning of the developing vasculature. Dev Cell. 2004; 7:117–23. [PubMed: 15239959]
34. Kim J, Oh WJ, Gaiano N, Yoshida Y, Gu C. Semaphorin 3E-Plexin-D1 signaling regulates VEGF function in developmental angiogenesis via a feedback mechanism. Genes Dev. 2011; 25:1399–411. [PubMed: 21724832]
35. Connolly SE, Hores TA, Smith LE, D'Amore PA. Characterization of vascular development in the mouse retina. Microvasc Res. 1988; 36:275–90. [PubMed: 2466191]
36. Baluk P, Morikawa S, Haskell A, Mancuso M, McDonald DM. Abnormalities of basement membrane on blood vessels and endothelial sprouts in tumors. Am J Pathol. 2003; 163:1801–15. [PubMed: 14578181]
37. Eelen G, de Zeeuw P, Simons M, Carmeliet P. Endothelial cell metabolism in normal and diseased vasculature. Circ Res. 2015; 116:1231–44. [PubMed: 25814684]
38. Simons M, Eichmann A. Molecular controls of arterial morphogenesis. Circ Res. 2015; 116:1712–24. [PubMed: 25953926]
39. Fischer A, Gessler M. Delta-Notch–and then? Protein interactions and proposed modes of repression by Hes and Hey bHLH factors. Nucleic Acids Res. 2007; 35:4583–96. [PubMed: 17586813]
40. Kopan R, Ilagan MX. The canonical Notch signaling pathway: unfolding the activation mechanism. Cell. 2009; 137:216–33. [PubMed: 19379690]
41. De Strooper B, Saftig P, Craessaerts K, Vanderstichele H, Guhde G, Annaert W, Von Figura K, Van Leuven F. Deficiency of presenilin-1 inhibits the normal cleavage of amyloid precursor protein. Nature. 1998; 391:387–90. [PubMed: 9450754]
42. Kimberly WT, LaVoie MJ, Ostaszewski BL, Ye W, Wolfe MS, Selkoe DJ. Gamma-secretase is a membrane protein complex comprised of presenilin, nicastrin, Aph-1, and Pen-2. Proc Natl Acad Sci U S A. 2003; 100:6382–7. [PubMed: 12740439]
43. Wolfe MS, Xia W, Ostaszewski BL, Diehl TS, Kimberly WT, Selkoe DJ. Two transmembrane aspartates in presenilin-1 required for presenilin endoproteolysis and gamma-secretase activity. Nature. 1999; 398:513–7. [PubMed: 10206644]

44. Abad-Rodriguez J, Ledesma MD, Craessaerts K, Perga S, Medina M, Delacourte A, Dingwall C, De Strooper B, Dotti CG. Neuronal membrane cholesterol loss enhances amyloid peptide generation. J Cell Biol. 2004; 167:953–60. [PubMed: 15583033]
45. Simons K, Ehehalt R. Cholesterol, lipid rafts, and disease. J Clin Invest. 2002; 110:597–603. [PubMed: 12208858]
46. He G, Luo W, Li P, Remmers C, Netzer WJ, Hendrick J, Bettayeb K, Flajolet M, Gorelick F, Wennogle LP, Greengard P. Gamma-secretase activating protein is a therapeutic target for Alzheimer's disease. Nature. 2010; 467:95–8. [PubMed: 20811458]
47. Rubin EM, Ishida BY, Clift SM, Krauss RM. Expression of human apolipoprotein A-I in transgenic mice results in reduced plasma levels of murine apolipoprotein A-I and the appearance of two new high density lipoprotein size subclasses. Proc Natl Acad Sci U S A. 1991; 88:434–8. [PubMed: 1703299]
48. Yvan-Charvet L, Pagler T, Gautier EL, Avagyan S, Siry RL, Han S, Welch CL, Wang N, Randolph GJ, Snoeck HW, Tall AR. ATP-binding cassette transporters and HDL suppress hematopoietic stem cell proliferation. Science. 2010; 328:1689–93. [PubMed: 20488992]
49. Simons M. Angiogenesis: where do we stand now? Circulation. 2005; 111:1556–66. [PubMed: 15795364]
50. Losordo DW, Dimmeler S. Therapeutic angiogenesis and vasculogenesis for ischemic disease: part II: cell-based therapies. Circulation. 2004; 109:2692–7. [PubMed: 15184293]
51. Losordo DW, Dimmeler S. Therapeutic angiogenesis and vasculogenesis for ischemic disease. Part I: angiogenic cytokines. Circulation. 2004; 109:2487–91. [PubMed: 15173038]
52. Bodnar JS, Chatterjee A, Castellani LW, Ross DA, Ohmen J, Cavalcoli J, Wu C, Dains KM, Catanese J, Chu M, Sheth SS, Charugundla K, Demant P, West DB, de Jong P, Lusis AJ. Positional cloning of the combined hyperlipidemia gene Hyplip1. Nat Genet. 2002; 30:110–6. [PubMed: 11753387]
53. Peloso GM, Demissie S, Collins D, Mirel DB, Gabriel SB, Cupples LA, Robins SJ, Schaefer EJ, Brousseau ME. Common genetic variation in multiple metabolic pathways influences susceptibility to low HDL-cholesterol and coronary heart disease. J Lipid Res. 2010; 51:3524–32. [PubMed: 20855565]
54. Chung AS, Ferrara N. Developmental and pathological angiogenesis. Annu Rev Cell Dev Biol. 2011; 27:563–84. [PubMed: 21756109]
55. Carmeliet P, Jain RK. Molecular mechanisms and clinical applications of angiogenesis. Nature. 2011; 473:298–307. [PubMed: 21593862]
56. Anand S, Cheresh DA. Emerging Role of Micro-RNAs in the Regulation of Angiogenesis. Genes Cancer. 2011; 2:1134–8. [PubMed: 22866204]
57. Urano Y, Hayashi I, Isoo N, Reid PC, Shibasaki Y, Noguchi N, Tomita T, Iwatsubo T, Hamakubo T, Kodama T. Association of active gamma-secretase complex with lipid rafts. J Lipid Res. 2005; 46:904–12. [PubMed: 15716592]
58. Ehehalt R, Keller P, Haass C, Thiele C, Simons K. Amyloidogenic processing of the Alzheimer beta-amyloid precursor protein depends on lipid rafts. J Cell Biol. 2003; 160:113–23. [PubMed: 12515826]
59. Park IH, Hwang EM, Hong HS, Boo JH, Oh SS, Lee J, Jung MW, Bang OY, Kim SU, Mook-Jung I. Lovastatin enhances Abeta production and senile plaque deposition in female Tg2576 mice. Neurobiol Aging. 2003; 24:637–43. [PubMed: 12885571]
60. Burns M, Duff K. Cholesterol in Alzheimer's disease and tauopathy. Ann N Y Acad Sci. 2002; 977:367–75. [PubMed: 12480774]
61. Karten B, Vance DE, Campenot RB, Vance JE. Cholesterol accumulates in cell bodies, but is decreased in distal axons, of Niemann-Pick C1-deficient neurons. J Neurochem. 2002; 83:1154–63. [PubMed: 12437586]
62. Vetrivel KS, Cheng H, Kim SH, Chen Y, Barnes NY, Parent AT, Sisodia SS, Thinakaran G. Spatial segregation of gamma-secretase and substrates in distinct membrane domains. J Biol Chem. 2005; 280:25892–900. [PubMed: 15886206]
63. Pasula S, Cai X, Dong Y, Messa M, McManus J, Chang B, Liu X, Zhu H, Mansat RS, Yoon SJ, Hahn S, Keeling J, Saunders D, Ko G, Knight J, Newton G, Luscinskas F, Sun X, Towner R, Lupu

F, Xia L, Cremona O, De Camilli P, Min W, Chen H. Endothelial epsin deficiency decreases tumor growth by enhancing VEGF signaling. J Clin Invest. 2012; 122:4424–38. [PubMed: 23187125]

NOVELTY AND SIGNIFICANCE

What Is Known?

- Increased blood vessel formation following cardiac ischemia contributes to improved cardiac recovery.
- ApoA-I binding protein (AIBP), a secreted protein, accelerates cholesterol efflux from endothelial cells, disrupts lipid rafts and impairs raft-associated VEGFR2 signaling, thereby restricting angiogenesis.
- Notch signaling counteracts VEGFR2 signaling, inhibits angiogenesis and stabilizes blood vessels.
- Notch activation entails its cleavage by γ-secretase, release of the intracellular domain and activation of a transcriptional program.

What New Information Does This Article Contribute?

- AIBP-mediated disruption of lipid rafts relocates Notch1 and γ-secretase from lipid rafts to nonraft domains.
- Increased localization of Notch1 and γ-secretase in the non-raft domains facilitates Notch1 cleavage and its activation.
- AIBP deficiency in mice attenuates Notch signaling.
- AIBP knockout augments retinal and pathological angiogenesis in mice.
- Expression level of AIBP in the heart is increased in patients with ischemic cardiomyopathy.

Angiogenesis is essential for tissue remodeling and repair following cardiac ischemia. Treatments that improve blood vessel formation holds great promise for patients with coronary artery disease. We previously found that the secreted protein, AIBP, limits angiogenesis via modulation of cholesterol metabolism. In this paper, we generated AIBP knockout mice and found that, consistent with our prior study, loss of AIBP increased developmental retinal angiogenesis and pathological angiogenesis in a murine hindlimb ischemia model. Furthermore, we showed that cardiac AIBP expression is increased in human ischemic cardiomyopathy. Our findings of AIBP-regulated angiogenesis may guide new treatment strategies that bolster angiogenesis in the pathological conditions.

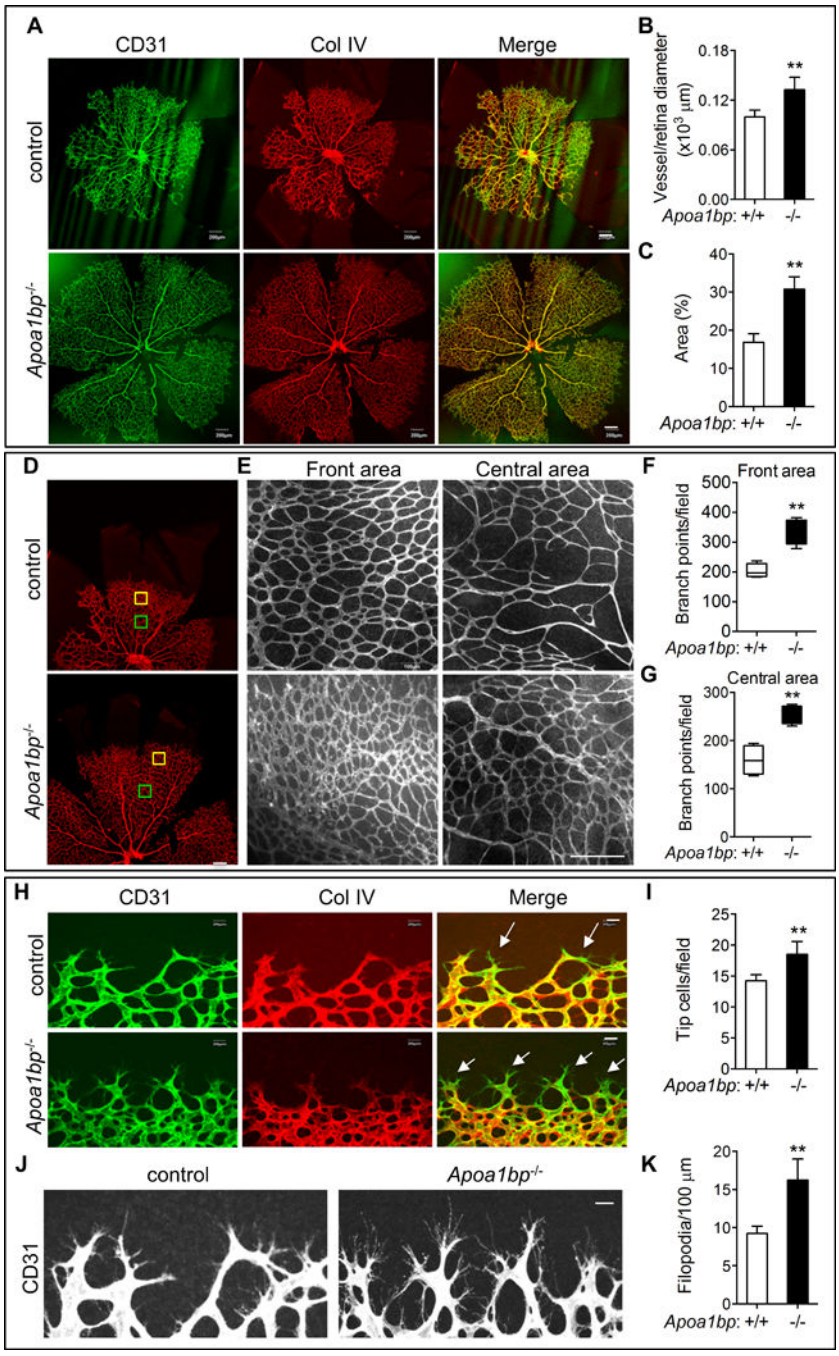

Figure 1. Retinal angiogenesis in *Apoa1bp* knockout mice

Retinas were isolated from P5 *Apoa1bp*$^{-/-}$ mice and their control littermates and whole mount immunostaining performed for CD31 (green) and Collagen (Col) IV (red). Confocal images of retinas (A) and the quantification of vessel and retina diameter (B) and vessel area (C). (D) The front and central areas of retinas analyzed are outlined in yellow and green. (E) Enlarged areas of yellow and green squares in D. Quantification of branch points in the front (F) and the central areas (G). (H and I) Tip cells and the quantification. Arrows show tip

cells. (J and K) Filopodia extension and the quantification. Mean ± SD; n=3. **, $p<0.01$. Scale bar: A, D, and E: 200 μm; H and J: 20 μm.

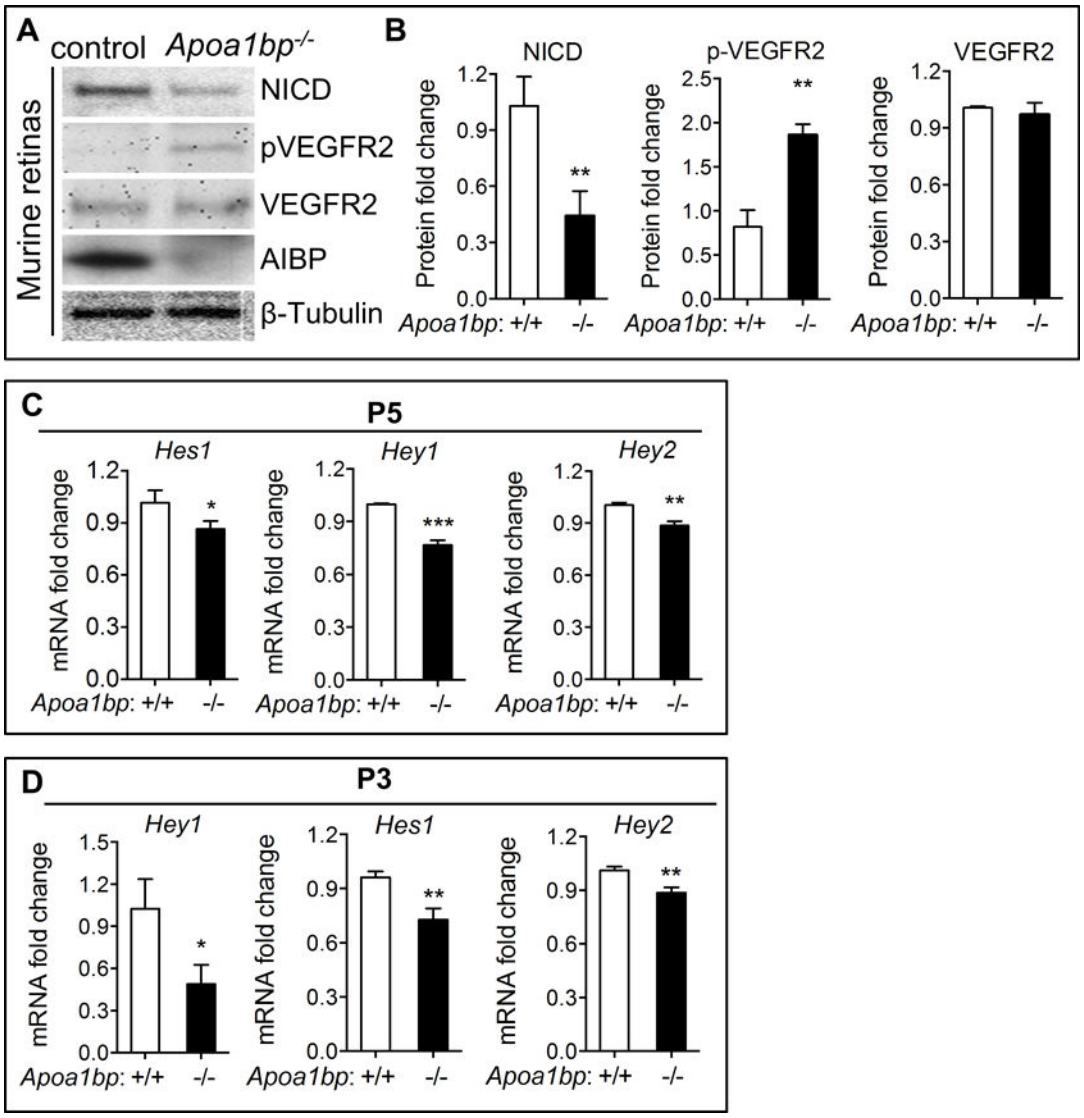

Figure 2. AIBP regulates Notch signaling in retinal angiogenesis

(A) Western blot analysis of NICD, phospho-VEGFR2 (pVEGFR2), and total VEGFR2 in the retinas of P5 AIBP knockout neonatal mice and their control littermates. (B) Quantification of A. The Y axis shows relative protein levels of NICD normalized to β-tubulin. Quantitative RT-PCR analysis of the Notch downstream target Hey1, Hey2 and Hes1 gene expression in *Apoa1bp*$^{-/-}$ and control retinas at P5 (C) and P3 (D). Mean ± SD; n=3. *, p<0.05; **, p<0.01; ***, p<0.001.

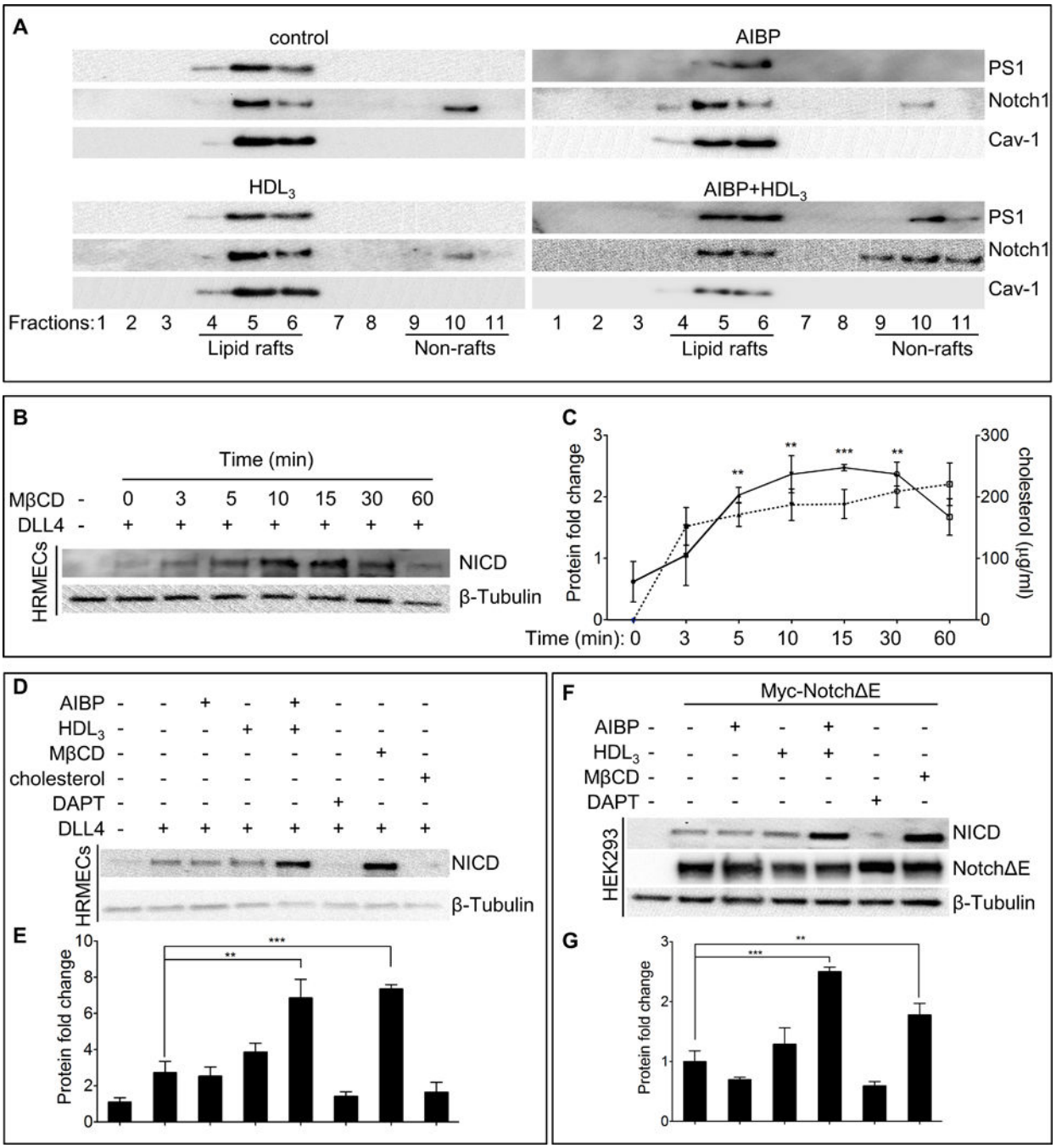

Figure 3. AIBP regulates Notch signaling through its effect on γ-secretase localization

(A) The distribution of γ-secretase and Notch1 in lipid rafts (fractions 4–6) and non-lipid rafts (fractions 9–11). HRMECs were incubated with 0.1 μg/ml AIBP, 50 μg/ml HDL_3, or their combination for 4 hours, and were disrupted and separated into lipid raft and non-lipid raft fractions by ultracentrifugation. Immunoblots of presenilin1 (PS1) and Notch1 were shown. (B) MβCD effect on Notch activation. HRMECs were seeded onto a 6-well plate precoated with or without 0.5 μg/ml recombinant DLL4 and followed by treatment with 10 mM MβCD for the indicated times. To ensure cells received equal DLL4 stimulation time,

the treatment was started at different time so as to harvest the cells simultaneously for immunoblotting of NICD. (C) Quantification of NICD protein levels in B (solid line) and measurements of free cholesterol content (dash line) removed from HRMECs with MβCD treatment. (D) AIBP and HDL_3 effect on Notch activation. HRMECs were seeded as in B, followed by treatment with AIBP (0.1 μg/ml), HDL_3 (50 μg/ml), AIBP/HDL_3 combination for 4 hours, with 20 μM DAPT (γ-secretase inhibitor) for 24 hours, with 10mM MβCD for 10 min, or with 10 μg/ml water-soluble cholesterol for 2 hours. The different treatments were started at various time so as to lyse the cells simultaneously for western blot of NICD. (E) Quantification of NICD proteins in D. (F) AIBP and HDL_3 effect on γ-secretase activity in HEK293 cells. HEK293 cells were transfected with NotchΔE or a control empty plasmid. After 48 hours, the resulting cells were treated as in D and used for immunoblots as indicated. NotchΔE was detected using anti-Myc Ab. (G) Quantification of F. The relative values of NICD/NotchΔE/ β-tubulin were normalized to that of control and the resulting numbers were used to generate the graph. Mean ± SD; the experiments were done with 3 independent repeats. In all panels: **, $p<0.01$; ***, $p<0.001$.

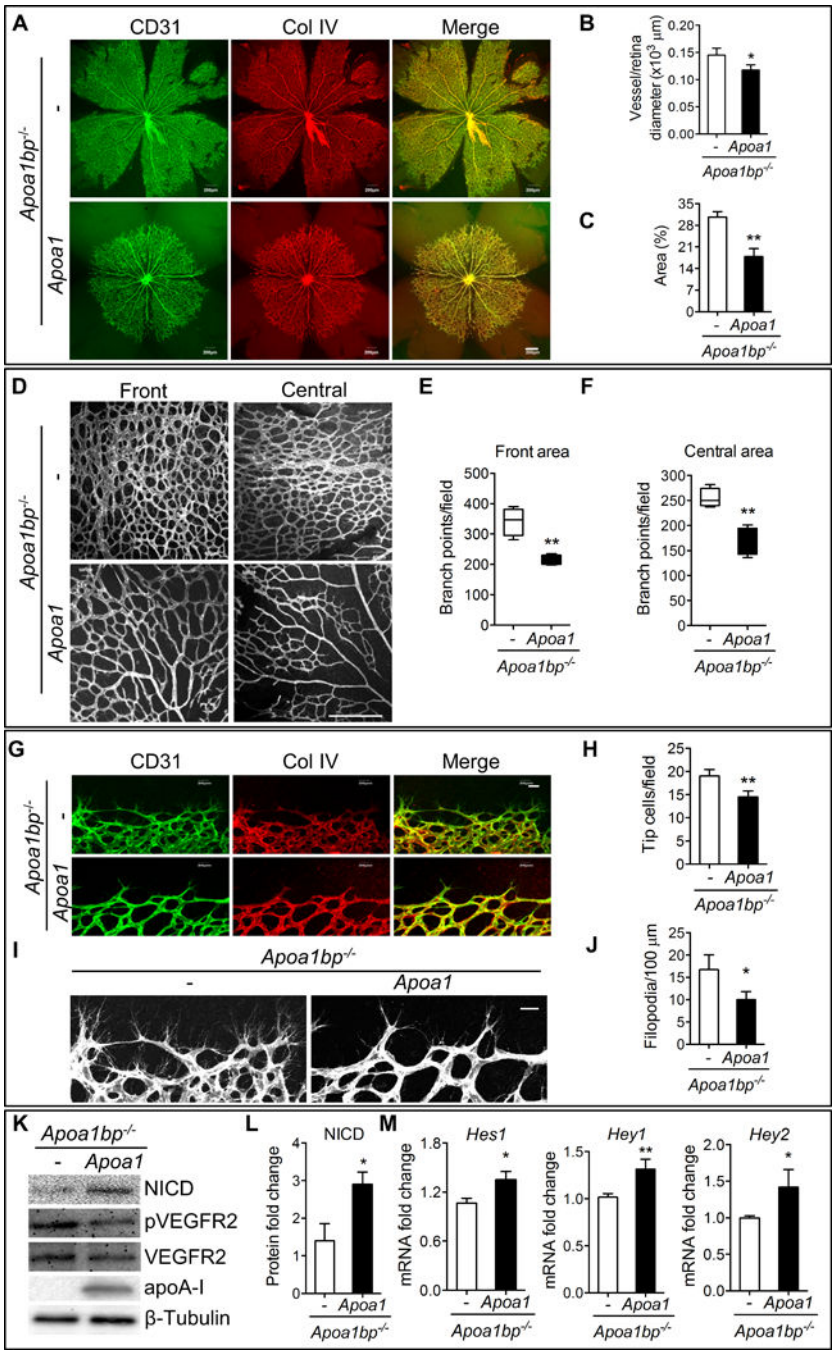

Figure 4. Rescue effect of increased HDL levels on angiogenesis and Notch signaling in AIBP null retinas

Retinas were isolated from *Apoa1bp*$^{-/-}$ *Apoa1*^{Tg} and control *Apoa1bp*$^{-/-}$ mice at P5 and whole mount immunostaining of CD31 (green) and Col IV (red) was performed. (A) Confocal images of retinas. Quantification of vessel and retina diameter (B) and vessel area (C). Retinal vasculature (D) and the quantification of branch points in the front areas (E) and central areas (F). (G and H) Tip cells and the quantification. (I and J) Filopodia extension and the quantification. (K) NICD, phospho-VEGFR2 (pVEGFR2), and total VEGFR2 protein levels in P5 retinas from *Apoa1bp*$^{-/-}$ *Apoa1*^{Tg} and control *Apoa1bp*$^{-/-}$ mice. (L)

Quantification of NICD protein levels in K. (M) Quantitative RT-PCR analysis of the Notch downstream *Hey1*, *Hey1* and *Hes2* gene expression in the retinas from $Apoa1bp^{-/-}Apoa1^{Tg}$ and $Apoa1bp^{-/-}$ mice at P5. Mean ± SD, n=3; *, $p<0.05$; **, $p<0.01$. Scale bar: A and D: 200 μm; G and I: 20 μm.

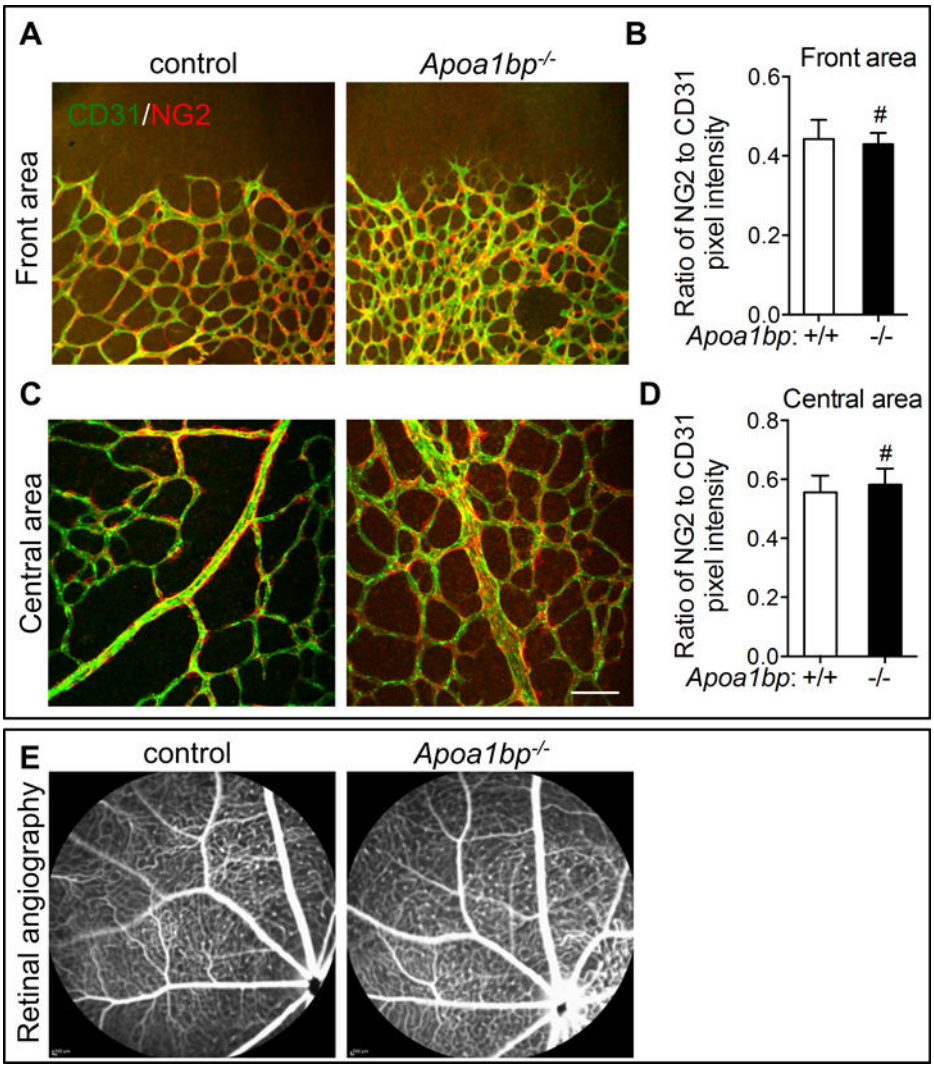

Figure 5. Vascular integrity in *Apoa1bp*$^{-/-}$ mice

Immunostaining of CD31 (green) and NG2 (red) in the front areas (A and B) and the central area (C and D) of the retinas from P5 *Apoa1bp*$^{-/-}$ neonatal mice or their control littermates and the quantification results of NG2 fluorescence intensity (B and D). (E) Representative Fluorescein Angiography images of 10-month *Apoa1bp*$^{-/-}$ and WT littermates (n=5 for AIBP KO and n=3 for WT control). For A–D, Mean ± SD; n=3. Scale bar: 100 μm. #, not significant.

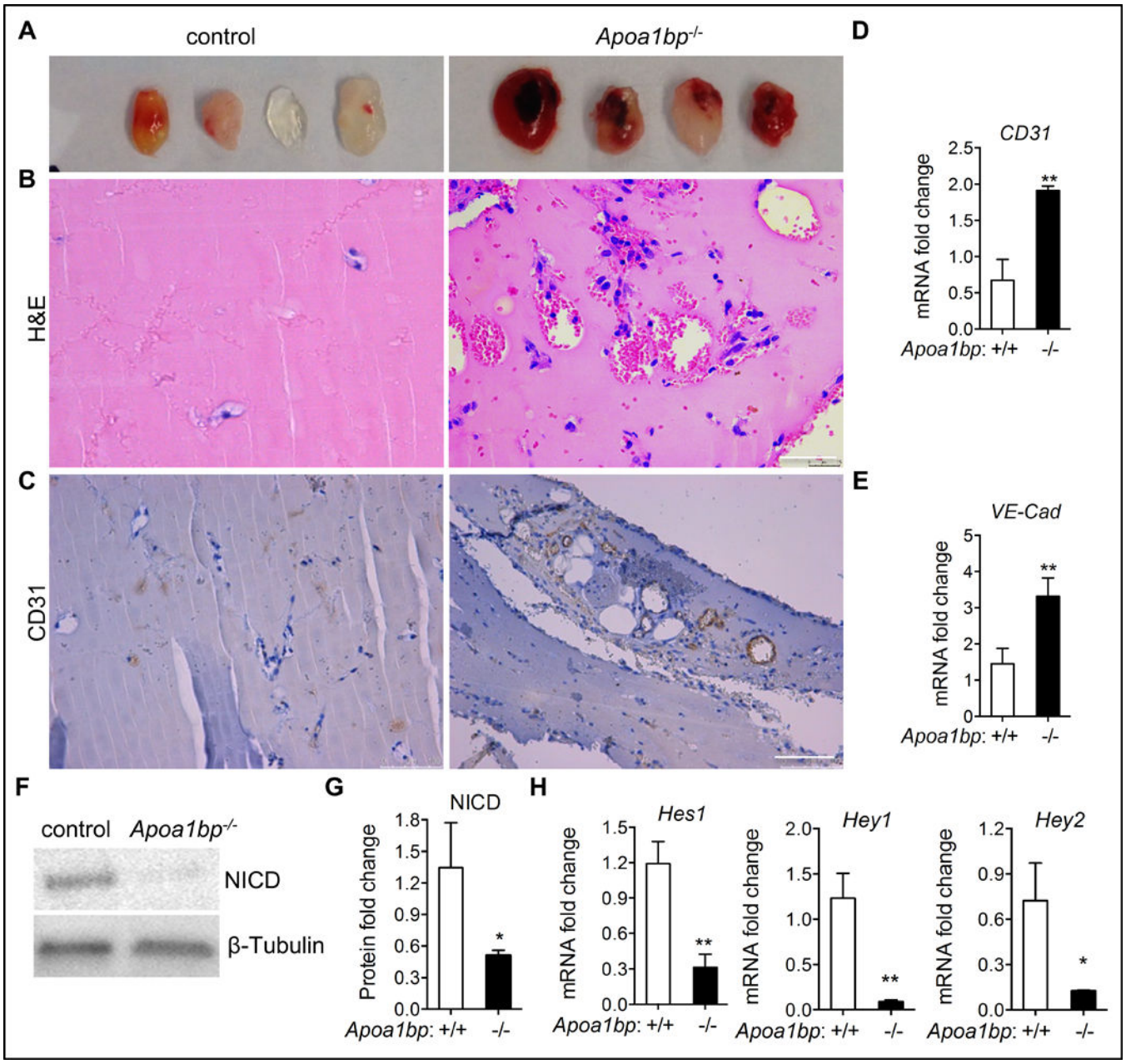

Figure 6. AIBP effect on neovessel formation in subcutanously implanted Matrigel plugs

(A) Images of Matrigel plugs retrieved from *Apoa1bp*$^{-/-}$ or control mice. Matrigel plugs were PFA-fixed, sectioned and subjected to H&E staining (B) and CD31 immunohistochemistry (C). Note that substantial amount of red blood cells were present in the Matrigel plugs from *Apoa1bp*$^{-/-}$ mice. (D and E) Quantitative RT-PCR analysis of EC gene markers CD31 and VE-cadherin (VE-Cad). Western blot of NICD expression (F), quantification of NICD protein levels in F (G) and qRT-PCR analysis of the Notch downstream gene expression (H) in the Matrigel plugs from *Apoa1bp*$^{-/-}$ or control mice. Mean ± SD; n=4, *, $p<0.05$; **, $p<0.01$. Scale bar: B, 50 μm; C: 100 μm.

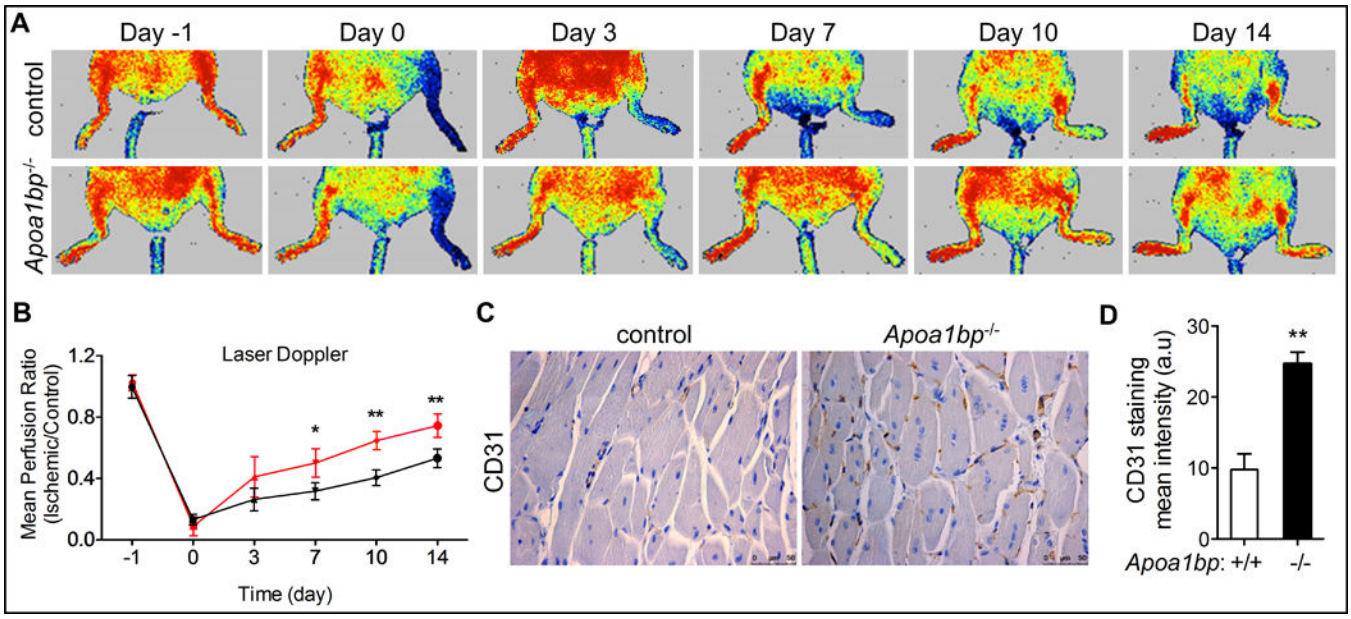

Figure 7. Laser Doppler Blood Perfusion (LDBP) imaging of control and AIBP KO mice

(A) Mice were subjected to hindlimb ischemia and representative Laser Doppler images were shown at the indicated time points. Arrows point to the ischemic limbs. (B) Quantitative assessment of limb perfusion. The results from AIBP KO mice are shown in red. (C) IHC analysis of CD31 staining in the ischemic tissue from control or AIBP KO mice. (D) Quantification of CD31 staining in C. Scale bar: 50 μm. Mean ± SE; n=8 in each group, *, $p<0.05$; **, $p<0.01$. The statistical analysis was done using one-way ANOVA.

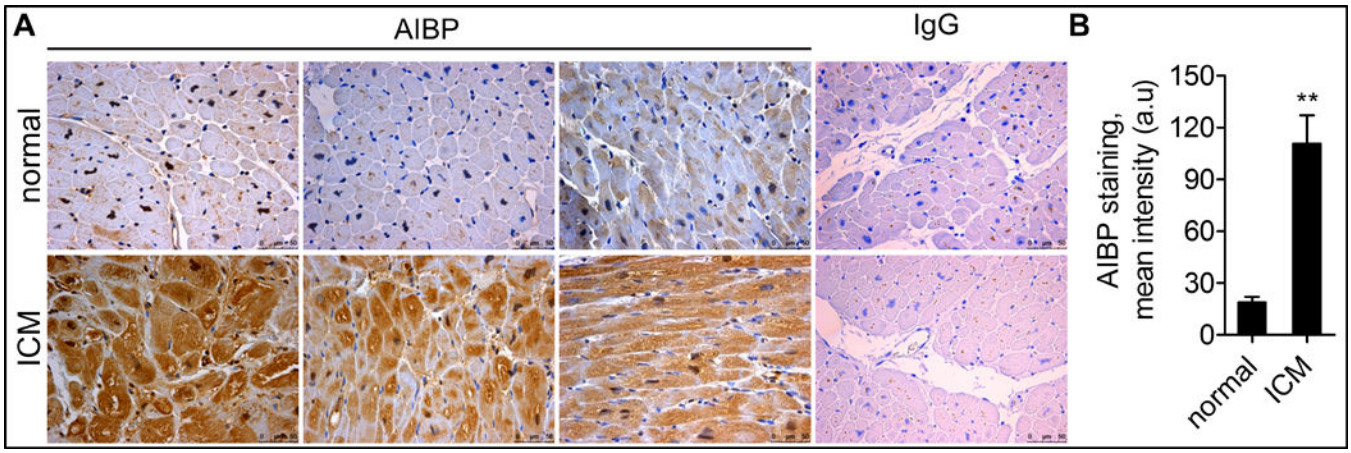

Figure 8. AIBP expression in myocardial tissue from normal subjects or those with ICM

(A) Human normal and ICM tissues were stained with AIBP antibody or control IgG, and further with a counterstain of the nuclei to visualize the myocardium. (B) The quantified data were shown on the right. Scale bar: 50 μm. **, $p<0.01$.